

Electrostatic and parallel-magnetic-field tuned two-dimensional superconductor-insulator transitions

Kevin A. Parendo, K. H. Sarwa B. Tan, and A. M. Goldman

School of Physics and Astronomy, University of Minnesota, Minneapolis, Minnesota 55455, USA

(Received 29 December 2005; revised manuscript received 3 March 2006; published 30 May 2006)

The two-dimensional superconductor-insulator transition in disordered ultrathin amorphous bismuth films has been tuned both by electrostatic electron doping using the electric field effect and by the application of parallel magnetic fields. Electrostatic doping was carried out in zero and nonzero magnetic fields, and magnetic tuning was conducted at multiple strengths of electrostatically induced superconductivity. The various transitions were analyzed using finite size scaling to determine their critical exponent products. For the electrostatically tuned transition, the exponent product $\nu z = 0.7 \pm 0.1$, using data from intermediate temperatures down to 60 mK. Here ν is the correlation length exponent and z is the dynamical critical exponent. In the case of electrostatically tuned transitions in field, and the field-tuned transitions at various values of electrostatically induced superconductivity, scaling was successful with $\nu z = 0.65 \pm 0.1$ from intermediate temperatures down to about 100 or 150 mK. The parallel critical magnetic field, B_c , increased with electron transfer as $(\Delta n - \Delta n_c)^{0.33}$, and the critical resistance decreased linearly with Δn . However, at lower temperatures, in the insulating regime, the resistance became larger than expected from extrapolation of its temperature dependence at higher temperatures, and scaling failed. These observations imply that although the electrostatic and parallel magnetic-field-tuned superconductor-insulator transitions would appear to belong to the same universality class and to be delineated by a robust phase boundary that can be crossed either by tuning Δn or B , in the case of the field-tuned transition at the lowest temperatures, some different type of physical behavior turns on in the insulating regime.

DOI: [10.1103/PhysRevB.73.174527](https://doi.org/10.1103/PhysRevB.73.174527)

PACS number(s): 74.40.+k, 73.43.Nq, 74.78.-w, 74.78.Db

I. INTRODUCTION

Continuous quantum phase transitions are transitions at absolute zero in which the ground state of a system is changed by varying a parameter of the Hamiltonian.^{1,2} The transitions between superconducting and insulating behavior in two-dimensional superconductors tuned by magnetic field or disorder (thickness) are believed to be such transitions. Early experiments and theories seemed to support a picture of only two ground states. Historically, the first theoretical approach to the superconductor-insulator (SI) transition was based on Cooper pairing being suppressed by the enhancement of the Coulomb repulsion between electrons with increasing disorder.³⁻⁵ In effect, the order parameter would be suppressed to zero in the insulating regime. The absence of a gap in the density of states in tunneling studies of the insulating regime has been interpreted as evidence for a zero superconducting order parameter amplitude in the insulating regime.⁶ Another approach to the SI transition was based on the transition being governed by phase fluctuations.⁷⁻⁹ In this “dirty Boson model,” the insulator is a vortex condensate with localized Cooper pairs, in contrast with the superconductor, which is a Cooper pair condensate with localized (pinned) vortices. Elaborations on this model have included effects of fermionic degrees of freedom.¹⁰ If phase fluctuations are pair breaking and destroy the superconducting energy gap, then this picture would also be consistent with the tunneling studies.

The three conventional approaches to the tuning of SI transitions all involve uncontrolled aspects of morphology. In the first method, a relatively thick (~ 100 Å) superconducting film is produced and magnetic fields are applied to

quench the superconductivity. These films are two dimensional in the sense that the coherence length and penetration depth are much greater than the films’ thicknesses. In this approach, the strength of the vortex pinning, which depends on the nature of the disorder, may determine the outcome of the measurements. In some measurements on films with relatively low sheet resistances,¹¹ the transition can also be described using quantum corrections to conductivity¹² and may not be quantum critical at all.¹³ In a second approach, the thickness of a film is increased in small increments, tuning from insulator to superconductor.¹⁴⁻¹⁶ However, films of different thicknesses may have different morphologies. In a third method, which has been used in some studies of In_2O_3 films, an insulating film is thermally annealed to produce superconductivity.^{17,18} However, thermal annealing may involve the alteration of morphology and chemical composition.

Successful finite-size scaling analyses with film thickness or magnetic field as tuning parameters have resulted in critical exponent products, νz , in the range of 1.2 to 1.4,^{11,19-22} which have been suggested to result from the transition being dominated by percolative effects,^{23,24} as this number is close to the exponent in two-dimensional (2D) percolation. One investigation of a perpendicular field tuned transition has yielded 0.7 as the product.²⁰

The simple two-ground state picture has been challenged in recent work, which appears to indicate that there is an extended intermediate metallic regime over an extended range of the tuning parameter. The physical evidence for such a regime is that resistances become independent of temperature at the lowest temperatures both in perpendicular field tuned transitions²⁵ and in thickness-tuned transitions.²⁶

In the case of the magnetic field experiments, the metallic regime abruptly disappears as the magnetic field is reduced, leading to true superconductivity. This is further evidence of possible sample inhomogeneity. There are several theories that describe an intermediate metallic regime^{27–29} in homogeneous samples. However it is not established that this regime is indeed intrinsic, and is not a consequence of either sample inhomogeneity, or the failure to cool a film. In overtly granular systems there is a clear intermediate metallic regime that is found at temperatures in excess of 1 K that is probably intrinsic.^{15,30}

Another phenomenon reported by a number of groups is the appearance of a large peak in the resistance vs magnetic field at fields in excess of the critical field for the SI transition. This has been observed in superconducting amorphous In_2O_3 and TiN films,^{13,31–37} or intrinsically insulating amorphous Be films.³⁸ With the exception of the work of Gantmakher *et al.*,³⁹ most of these studies have been conducted in perpendicular magnetic fields. No quantitative theoretical explanation has yet been put forward to explain these very large values of resistance found on the insulating side of the SI transition. It is not clear that this phenomenon is an intrinsic property of a homogeneous material or results from some mesoscale inhomogeneity.

Since there are important concerns about morphology and disorder in the above-mentioned studies, the aim of the present work was to attempt to clarify these issues by studying SI transitions in which the level of physical disorder was fixed, and in which the outcome was not dependent upon the degree of vortex pinning. This is possible by inducing superconductivity in an insulator by electrostatic doping using the electric field effect⁴⁰ and then applying a parallel magnetic field to drive the film back into the insulating state. The same level of chemical and physical disorder may be shared by both the intrinsic insulating state, and the insulating state in which the electrostatically induced superconductivity is quenched by magnetic field. We will present arguments to the effect that electrostatic doping does not alter physical or chemical disorder, but changes the coupling constant that determines superconductivity. Parallel magnetic fields destroy superconductivity by polarizing spins, but not by inducing vortices. These studies were carried out in a very carefully shielded dilution refrigerator to enhance the chances that very low heat capacity films would cool.

The experimental approach used in this work will be described in Sec. II. In Sec. III the various results will be presented. Sections IV and V contain a discussion of these results along with conclusions that can be drawn.

II. EXPERIMENTAL APPROACH

These investigations were carried out in a geometry in which a SrTiO_3 (STO) crystal served as both a substrate and a gate insulator in a field effect transistor configuration. To prepare this device, first a small section of the unpolished back surface of a $500\ \mu\text{m}$ thick single crystal of (100) STO substrate was mechanically thinned⁴¹ *ex situ*, resulting in this surface and the epi-polished front surface being parallel and separated by $45 \pm 5\ \mu\text{m}$. A $0.5\ \text{mm}$ by $0.5\ \text{mm}$, $1000\ \text{\AA}$ thick,

Pt “gate” electrode was deposited *ex situ* onto the thinned section of the back surface directly opposite the eventual location of the measured square of film. Platinum electrodes, $100\ \text{\AA}$ thick, were also deposited *ex situ* onto the substrate’s epi-polished front surface to form a four probe measurement geometry. The substrate was then placed in a Kelvinox-400 dilution refrigerator/UHV deposition apparatus.⁴² A $10\ \text{\AA}$ thick underlayer of amorphous Sb and successive layers of amorphous Bi (*a*-Bi) were thermally deposited *in situ* under ultrahigh vacuum conditions (10^{-9} Torr) through shadow masks onto the substrate’s front surface. The distance between current electrodes was $2.5\ \text{mm}$ and the width was $0.5\ \text{mm}$. The substrate was held at about 7 K during the deposition process. Films grown in this manner are believed to be homogeneously disordered on a microscopic, rather than on a mesoscopic scale.¹⁴

A Keithley 487 voltage source was used to apply voltages between the film and the gate electrode. In essence, the film and the gate electrode formed a parallel plate capacitor with the thinned layer of STO serving as the dielectric spacer. Applying a positive voltage, V_G , to the gate electrode caused electrons to be transferred into the film. Since STO crystals have very large dielectric constants at temperatures below 10 K ($\sim 20\ 000$), and since the substrate was greatly reduced in thickness, the gate voltage produced large electric fields that facilitated large transfers of electrons. Since the dielectric constant of STO is known to vary strongly with electric field, an analysis was performed that yielded the relationship between V_G and the areal density of added electrons, Δn , for this substrate and film sequence. Bhattacharya *et al.* deposited a Pt film and gate electrode onto a $35\ \mu\text{m}$ thick STO substrate, charged a film to various gate voltages and measured the number of electrons that exited the film each time it was quickly discharged, as shown in Fig. 3 of that work.⁴¹ The calibration that was performed at 2 K was repeated on the same substrate with more data points than shown in that publication. This provided a generic calibration of charge transfer versus electric field for thin STO substrates. The geometries of the substrates used in that work and in the work discussed here were measured, and from this information a calibration of Δn vs V_G for this film sequence was inferred. At positive gate voltages, transferred electron densities were found to be between 0 (at $V_G=0$) and $3.35 \times 10^{13}\ \text{cm}^{-2}$ (at $V_G=42.5\ \text{V}$). A calibration of Δn vs V_G was not performed by charging and discharging this *a*-Bi film because even slow ramping of gate voltage caused fairly large currents to flow in the film. Sudden, large discharges would probably cause very large currents to flow in the film. In a previous *a*-Bi film, application of very large currents irreversibly changed film properties, which we wished to avoid. In this film sequence, application of V_G above $42.5\ \text{V}$ did not change any measurement of film properties relative to those at $42.5\ \text{V}$.

The sample measurement lines were heavily filtered so as to minimize the electromagnetic noise environment of the film. The approach was to use RC filters at 300 K to attenuate 60 Hz noise, Spectrum Control #1216-001 π -section filters at 300 K (in series with $10\ \text{k}\Omega$ resistors) to attenuate radio frequency noise, and 2 m long Thermocoax cables⁴³ at the mixing chamber stage of the refrigerator to attenuate

GHz Johnson noise from warmer parts of the refrigerator. To avoid complications arising from this filtering, measurements were made using dc, rather than ac, methods. A 1 nA dc current, I , was applied to the films using a Keithley 220 current source. Voltage, V , was measured across the center-most 0.5 mm by 0.5 mm square of the film using a Keithley 182 voltmeter. The sheet resistance of the film, R , was taken to be V/I .

The films clearly fail to cool much below 60 mK, even though the dilution refrigerator cools to 7 mK. This is almost certainly due to the thermal load on the films that is caused by the residual noise environment, together with limitations on the thermal grounding of the electrical leads. It is very difficult to cool the electrons of a film at such low temperatures. Ultrathin films have a negligible heat capacity and since in this instance, they are not immersed in a cooling fluid, the mechanism for the electrons to cool is through their thermally (but not electrically) grounded leads and through contact of the film with the “thermal bath” of phonons in the film. At mK temperatures, however, electrons and phonons are known to decouple.⁴⁴ The mixing chamber cools to 7 mK, as verified by a ⁶⁰Co nuclear orientation thermometer. To determine the actual temperature of a film, we used its electrical resistance in the insulating regime as a thermometer. As will be discussed in Sec. III, a good fit to the temperature dependent resistance from 12 K down to 60 mK was an exponential activation form characteristic of 2D Mott variable range hopping. However, at 60 mK, $R(T)$ began to deviate from this form and eventually became independent of temperature as the mixing chamber approached 7 mK. This is consistent with the electrons of the film not cooling even while the mixing chamber continues to cool. Removal of the 60 Hz filtering raised the temperature at which the 9.60 Å thick film began to deviate from the Mott form at 140 mK; above this temperature, $R(T)$ was relatively unchanged. This suggests that the noise environment prevented the film from cooling after the removal of the filter. By an extension of this logic, we believe that, with the full filtering present, the residual noise environment prevented the film from cooling below about 60 mK.

Since *in situ* rotation of the sample into alignment perpendicular to the axis of the magnetic was not possible during this series of experiments, Hall effect measurements that could have yielded the intrinsic charge density were not performed. Electrons were stated by Buckel to be the charge carriers in *a*-Bi, from a determination of the Hall coefficient in relatively thick (~ 500 Å) films.⁴⁵ However, the sign of the Hall coefficient is known to lead to an erroneous determination of the sign of the charge carrier in amorphous semiconductors.⁴⁶ If *a*-Bi acted like a semiconductor in this regard, then holes would be the charge carriers, which would make it similar to most other superconductors. Thermopower measurements could accurately ascertain the sign of the of charge carriers in *a*-Bi.⁴⁶ Buckel’s Hall effect measurements yield estimates of areal charge densities of between 10^{14} and 10^{15} cm⁻² in metallic *a*-Bi films.

Careful attention was given to ensure that voltages were measured only while the film was in thermal equilibrium. Ramping V_G even at slow rates caused heating of the film because real currents flowed in the film in response to the

displacement currents that were induced by changing V_G . Ramping the magnetic field caused Eddy current heating. Lastly, it was found that the rate at which the film cooled and warmed in high magnetic fields decreased dramatically compared to the rate at low fields. Thus, the measurement procedure that was used involved ramping V_G and/or magnetic field to constant values and waiting long times (between three and six h) to fully cool the film to 60 mK. After this, voltages were measured as a function of temperature from 60 mK to 1 K in controlled steps using temperature feedback and long equilibration times (between 5 and 15 min per temperature). Appropriate equilibration times after ramping V_G , B , and T were determined by checking reproducibility, i.e., by taking measurements after longer wait times, with varying rates, and by recording voltage for many hours at stable temperatures while watching for drift that would signal behavior that was out of equilibrium.

In a quantum phase transition, the resistances of 2D films are expected to obey the finite size scaling functional form⁸

$$R/R_c = F(|K - K_c|/T^{1/\nu z}), \quad (1)$$

where F is an unknown function, K is the tuning parameter, K_c is the critical value of the tuning parameter, R_c is the critical resistance, ν is the correlation length critical exponent, and z is the dynamical critical exponent. To analyze data using this finite size scaling form, we first plotted isotherms of $R(K)$. A crossing point separates the insulating and superconducting phases, yielding the critical values R_c and K_c . As temperature becomes too high, subsequent isotherms will not cross at a single point (R_c, K_c), and these temperatures are then excluded from the analysis. After determining R_c and K_c , all of the parameters characterizing the scaling analysis are known except for the product νz . This product is then taken as the unknown, and R/R_c is plotted against $|K - K_c|/T^{-1/\nu z}$ for various values of νz . The value of νz that produces the best collapse of data is then the exponential product.

III. RESULTS

A. The intrinsic insulating regime

A sequence of *a*-Bi films was studied. As a function of increasing thickness, there were four thicknesses that were insulating and nine that were superconducting. Here we focus on the four insulating thicknesses that we refer to as “intrinsic” insulators. For data shown in Fig. 1, there was no gate bias and no applied magnetic field. The temperature dependence of the resistance, $R(T)$, at each thickness was consistent with Mott variable range hopping (VRH) conduction in 2D, as the best fits were of the form

$$R(T) = R_0 \exp([T_0/T]^{1/3}) \quad (2)$$

where the constants R_0 and T_0 are the resistance prefactor and the activation energy (in K), respectively. This is shown in the inset to Fig. 1. For the 9.69 Å and 9.91 Å thick films, data were available to verify this form up to 12 K. Unsuccessful attempts were made to fit $R(T)$ with hopping powers of 1/4, 1/2, 0.7, and 1 as well as the relationship expected

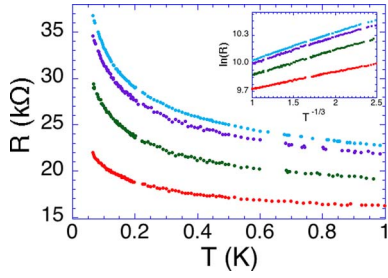


FIG. 1. (Color online) $R(T)$ for thicknesses of 9.60, 9.69, 9.91, and 10.22 Å (top to bottom in the curves in main figure and inset). Data for $\Delta n=0$, $B=0$, and T from 60 mK to 1 K, are shown as $R(T)$ (main) and $\ln(R)$ vs $T^{-1/3}$ (inset). T_0 and R_0 decrease with thickness, being 39, 32, 25, and 8 mK and 16406, 16001, 14317, and 13310 Ω , respectively.

for weak localization and electron-electron interactions

$$G \equiv 1/R = G_0 + k \ln(T/T_0) \quad (3)$$

where G is the conductance and k and T_0 are constants. Fits were not attempted in which the prefactor R_0 was taken to be temperature dependent.

Mott VRH conduction is found in strongly localized systems in the absence of Coulomb interactions between electrons. For this work, the absence of Coulomb interactions may be caused by screening of the electric fields in the film⁴⁷ because of proximity to the STO substrate, which has a very high dielectric constant.

B. Electrostatic tuning of the SI transition in zero magnetic field

In the case of the 10.22 Å thick film, which exhibited the highest conductance for the four intrinsically insulating thicknesses of the sequence, the addition of electrons to the film induced superconductivity. The evolution of this electrostatically tuned SI transition with charge transfer is shown in Fig. 2. With the charge transfer, $\Delta n=0$, $R(T)$ was well described by Mott hopping. With $\Delta n=0.85 \times 10^{13} \text{ cm}^{-2}$, the best fit from 60 mK to 1 K was that of a $\ln(T)$ dependence of the conductance on temperature as given in Eq. (3). This

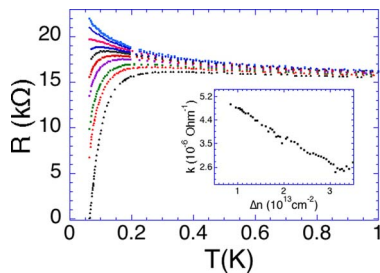


FIG. 2. (Color online) Resistance versus temperature at various values of Δn for the 10.22 Å thick film with $B=0$. Data are shown from 60 mK to 1 K. The values of Δn that are shown, from top to bottom, are 0, 0.62, 1.13, 1.43, 1.61, 1.83, 2.04, 2.37, 2.63, and $3.35 \times 10^{13} \text{ cm}^{-2}$. Forty four curves of $R(T)$ for other values of Δn are omitted from the plot for clarity. Inset: slope of $\ln(T)$ from Eq. (3), k vs Δn .

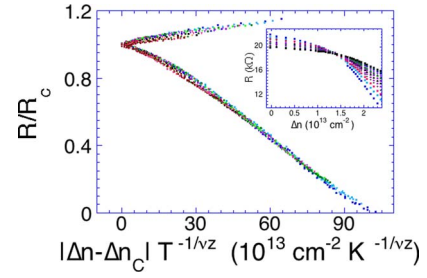


FIG. 3. (Color online) Finite size scaling plot for the 10.22 Å thick film with $B=0$, including data from 60 mK to 140 mK with Δn as the tuning parameter. Fifty four values of Δn between 0 and $3.35 \times 10^{13} \text{ cm}^{-2}$ were included. The best collapse of the data was for $\nu z=0.7$ with an uncertainty of ± 0.1 . Inset: $R(\Delta n)$ for isotherms between 60 mK and 140 mK.

was the first density at which $G(T)$ was definitely fit better by $\ln(T)$ than by the Mott hopping form given in Eq. (2). At larger values of Δn , as superconducting fluctuations became strong at lower temperatures, this $\ln(T)$ dependence remained the best fit at higher temperatures. With $\Delta n=3.35 \times 10^{13} \text{ cm}^{-2}$, the film was fully superconducting (within the scatter of our data) with the superconducting transition temperature $T_c=60$ mK. Superconducting fluctuations were strong between 60 mK and about 250 mK, and the conductance was best described by the $\ln(T)$ temperature dependence above 250 mK. The value of the slope of $\ln(T)$ is plotted as a function of Δn for superconducting curves in the inset to Fig. 2. The fact that the slope varies in a linear fashion with Δn is striking. The actual mechanism for this $\ln(T)$ dependence is unknown. We have previously suggested that it may be due to a combination of weak localization and electron-electron interactions despite the high value of film resistance.⁴⁰ If one assumed that only the electron-electron interaction contribution change, then this would imply that the Hartree screening parameter changed linearly with Δn , perhaps contributing to the inducing of superconductivity.

This transition was successfully analyzed using finite size scaling employing Δn as the tuning parameter. This suggests that the electrostatically tuned SI transition is a quantum phase transition. In the inset to Fig. 3 we show $R(\Delta n)$ for multiple isotherms between 60 mK and 140 mK. There is a distinct crossing point at the critical electron density, $\Delta n_c = 1.28 \times 10^{13} \text{ cm}^{-2}$ and the critical resistance, $R_c=19\,109 \Omega$. In the main part of Fig. 3, we show the scaling plot. The value of the critical exponent product νz that brings about the best collapse of data is 0.7 ± 0.1 . The range over which scaling is successful is from 60 mK to 140 mK.

The scaling analysis with uncorrected data appears to fail at temperatures above 140 mK because of the $\ln(T)$ dependence of the conductance in the normal state. It is possible to successfully extend the analysis up to 1 K if this dependence is first removed. This is done by assuming that there are two parallel conductance channels, one that gives the $\ln(T)$ dependence and the other that gives superconducting and insulating fluctuations. We then find the critical charge transfer to be at $\Delta n_c=0.85 \times 10^{13} \text{ cm}^{-2}$ since at this density $R(T)$ can be fit by $\ln(T)$ over the entire temperature range (from 60 mK to 1 K). The best fit to $G(T)$ at Δn_c is then written as

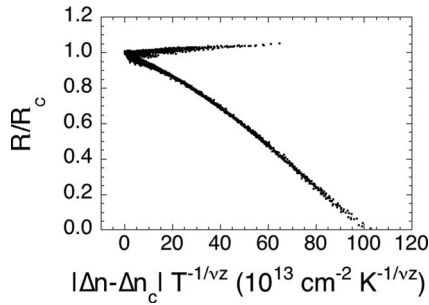


FIG. 4. Finite size scaling plot for the 10.22 Å thick film with $B=0$ including values of $R(T)$ from 60 mK to 1 K with Δn as a tuning parameter, having first removed the contributions to $R(T)$ from the conductance channel responsible for the $\ln(T)$ dependence. The best collapse of the data was for $\nu z=0.7$ with an uncertainty of ± 0.1 .

$G_{0c} + k_c \ln(T)$ and the critical resistance is the temperature independent part of the resistance at Δn_c , or $1/G_{0c}$. For each Δn , we subtracted $k_c \ln(T)$ from $G(T)$. After this, we determined the value of νz that minimized the error in data collapse on the scaling curves in the same manner as for the uncorrected data. All values of $R(T)$ from 60 mK to 1 K then successfully fell onto the scaling curves, as shown in Fig. 4. The critical exponent product remained at 0.7 ± 0.1 . The parallel conductance channel responsible for the $\ln(T)$ dependence is thus removed from the analysis using this procedure. This approach is perhaps more physical than that used by Gantmakher *et al.*²² in the study of perpendicular magnetic field tuned SI transitions of In_2O_3 films, where scaling was successful at the lowest temperatures, but a positive dR_c/dT at high temperatures prevented scaling. To broaden the temperature range they subtracted a linear temperature dependence from $R_c(T)$.

This SI transition appears to involve little change in the physical disorder, as determined by noting that the resistance at high temperatures ($T \geq 1$ K) changes very little as superconductivity develops. This resistance is related to the product of the Fermi wave vector, k_F , and the electronic mean free path, l . If $k_F l$ does not change much, then one can assume that disorder does not change much. In Fig. 5, we show the resistance at low temperature (120 mK) as a function of the resistance at 1 K for the electrostatic tuned transition and a previously reported thickness-tuned transition.²⁶ One can see that, as insulating behavior changes to superconducting behavior, the thickness-tuned transition takes place with a much larger change in the high temperature resistance than does the electrostatically tuned system. To further the idea that electrostatic doping adjusts electronic properties but not disorder, we note that for intrinsically superconducting films with transition temperatures between 1 and 4 K, the application of $V_G = \pm 50$ V shifted transition temperatures by as much as 40 mK, but these shifts were accompanied by very small changes in the resistance at 10 K (about 10–20 Ω for normal state resistances of 3–5 kΩ).

We note that data in Figs. 2 and 3 and part of the discussion in this section were previously reported,⁴⁰ but are included here with modifications. First, data are only shown down to 60 mK as that is now believed to be the lowest

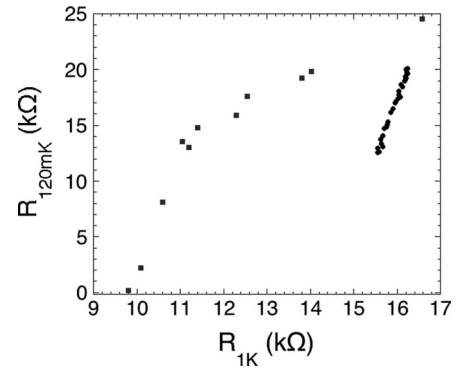


FIG. 5. Resistance at 1 K as a function of resistance at 120 mK for electrostatic (circles) and thickness (squares) tuned transitions. As superconductivity develops, the resistance at 1 K changes much more for thickness tuning than for electrostatic tuning.

temperature to which the film reliably cools. Second, data are shown, described, and analyzed in terms of Δn rather than V_G since Δn is the more physical variable. One consequence of this using Δn is that the coefficient, k , of $G \sim k \ln(T)$ depends linearly on Δn , as shown in the inset of Fig. 2, while in the previous publication it varied nonlinearly with V_G . Also, the scaling analysis shown in Fig. 3 has a much better collapse of data over a larger temperature range when conducted with Δn as the tuning parameter than when the analysis was conducted previously in terms of V_G .

C. Electrostatic tuning of the SI transition in a 2.5 T parallel magnetic field

Electrostatic tuning of the SI transition in the 10.22 Å thick film was carried out in a parallel magnetic field of 2.5 T. Resistance versus temperature at various values of B for this transition is shown in Fig. 6. The application of magnetic field to an ungated insulating film increased its activation energy. Adding electrons increased the film's conductivity and, at high enough density, induced a transition to superconductivity.

Comparing Figs. 2 and 6, a difference between the electrostatically tuned SI transitions in zero and nonzero mag-

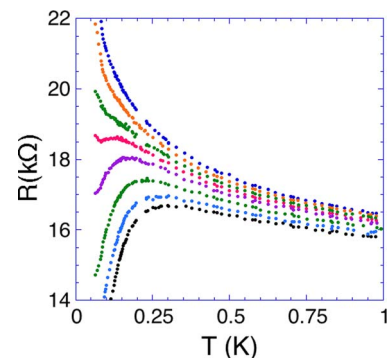


FIG. 6. (Color online) Resistance versus temperature at various values of Δn for the 10.22 Å thick film with $B=2.5$ T. Values of Δn shown are 0, 0.74, 1.28, 1.57, 1.87, 2.30, 2.74, and 3.13 $\times 10^{13} \text{ cm}^{-2}$, from top to bottom. Fifteen curves of $R(T)$ at other values of Δn have been omitted from the plot for clarity.

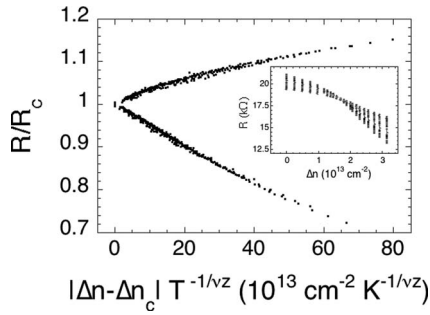


FIG. 7. Finite size scaling plot for the 10.22 Å thick film with $B=2.5$ T including values of $R(T)$ from 100 mK to 200 mK with Δn as the tuning parameter. Twenty three values of Δn between 0 and $3.13 \times 10^{13} \text{ cm}^{-2}$ were included. The best collapse of the data was for $\nu_z=0.65$ with an uncertainty of ± 0.1 . Inset: $R(\Delta n)$ for isotherms between 100 mK and 200 mK, exhibiting a well-defined crossing point at $\Delta n=1.7 \times 10^{13} \text{ cm}^{-2}$ and $R=18\,300 \text{ } \Omega$.

netic fields is evident: at low temperatures in finite field, near criticality, curves that appear to be heading towards zero resistance as temperature is lowered suddenly undergo a change in slope and appear to be insulating when extrapolated to the limit of zero temperature. Also, farther on the insulating side of the transition, the resistance at the lowest temperatures is larger than that expected from the extrapolation of $R(T)$ from higher temperatures. This is a more subtle effect that is not apparent from the $R(T)$ plot, but can be seen when data are plotted in the form expected for Mott VRH. We will refer to these effects as “excess resistance” since in both cases, resistance is higher than would be expected from extrapolation of $R(T)$ from higher temperature. These effects will be discussed in detail in Sec. III F.

A finite size scaling analysis was carried out for the electrostatically tuned transition in field. In the inset to Fig. 7, we show $R(\Delta n)$ for isotherms between 100 and 200 mK. A distinct crossing point is apparent, yielding $\Delta n_c=1.7 \times 10^{13} \text{ cm}^{-2}$ and $R_c=18\,300 \text{ } \Omega$. In the main body of Fig. 7, we show the scaling plot. The value of the exponent product that minimized the collapse of data was 0.65 ± 0.1 , which is slightly lower than the electrostatic tuned transition in zero field but is in agreement with it if the uncertainty of the analysis is taken into account. Data below 100 mK do not fall onto the scaling plot because of the excess resistance.

The successful scaling analysis implies that the system is moving towards insulating and superconducting ground states that are separated by a quantum critical point. The break down in scaling implies that instead of reaching this insulating ground state, one with a higher resistance is actually achieved.

D. Parallel magnetic field tuning of the SI transition

In the case of the 10.22 Å thick film, after superconductivity was induced by adding an areal density of carriers $\Delta n=3.35 \times 10^{13} \text{ cm}^{-2}$, superconductivity was quenched by a parallel magnetic field, and a detailed study of the parallel magnetic field tuned SI transition was conducted. In Fig. 8, we show this transition. With $B=0$, the superconducting tran-

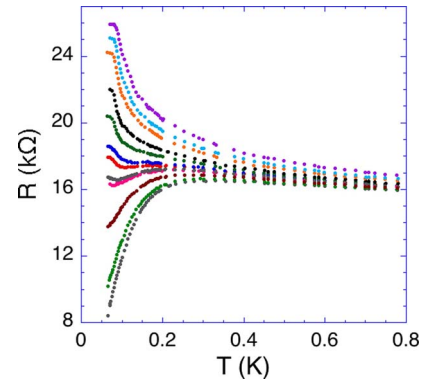


FIG. 8. (Color online) Resistance versus temperature at various values of B for an insulating film with superconductivity induced by a charge transfer $\Delta n=3.35 \times 10^{13} \text{ cm}^{-2}$. Values of B are 2 (bottom), 2.5, 3.5, 4.25, 4.375, 4.75, 5, 5.75, 6.5, 8, 9, and 11 T (top). Seven $R(T)$ curves for other values of B have been omitted from the plot for clarity.

sition temperature, $T_c=60$ mK (taken to be the highest temperature at which resistance is zero within the scatter due to noise), the mean field transition temperature (taken to be the temperature at which resistance is half of the normal state peak) is 90 mK, and the peak in $R(T)$ below which there are strong superconducting fluctuations is at 250 mK. The normal state, taken to be at temperatures in excess of that at which $R(T)$ exhibits a peak, is best described by a conductance that has a logarithmic temperature dependence. This superconductor at $B=0$ becomes an insulator at high fields that is again well described by 2D Mott VRH at temperatures greater than 130 mK.

Analysis of this transition using finite size scaling is successful over a wide range of temperature, provided that the regime of excess resistance discussed above is excluded from the analysis. The scaling analysis is shown in Fig. 9. The inset to Fig. 9 shows a set of isotherms of resistance vs field between 150 and 340 mK, which exhibits a distinct crossing point at $R_c=17\,285 \text{ } \Omega$ and $B_c=4.625 \text{ T}$. The value of the exponent product ν_z that minimized collapse of data is 0.65 ± 0.1 . Within the experimental uncertainty, this value is the same as that found for the electrostatically tuned transitions in zero field and 2.5 T.

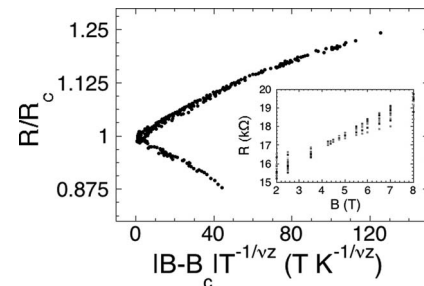


FIG. 9. Finite size scaling plot for the 10.22 Å thick film with $\Delta n=3.35 \times 10^{13} \text{ cm}^{-2}$ with B as the tuning parameter for $150 \text{ mK} < T < 340 \text{ mK}$. The best collapse of the data was for $\nu_z=0.65$ with an uncertainty of ± 0.1 . Inset: Isotherms of $R(B)$ at temperatures between 150 mK and 340 mK.

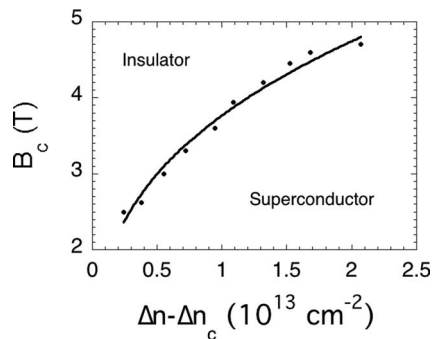


FIG. 10. Phase diagram of B_c vs $(\Delta n - \Delta n_c)$ for the 10.22 Å thick film. The best fit is by a power law with an exponent of 0.33.

E. Phase diagrams

We have carried out a systematic study of the parallel magnetic field tuned SI transition at various strengths of electrostatically induced superconductivity. The scaling procedure for the B -tuned transition for $\Delta n = 3.35 \times 10^{13} \text{ cm}^{-2}$ discussed in the previous section was repeated at $\Delta n = 1.66$, 2.25, and $2.80 \times 10^{13} \text{ cm}^{-2}$, yielding the same exponent product $\nu z = 0.65 \pm 0.1$.

At values of $\Delta n = 1.83$, 2.00, 2.40, 2.59, and 2.96 $\times 10^{13} \text{ cm}^{-2}$, $R(B)$ was measured at 100 and 120 mK and the crossing points determined. These temperatures were within the range used to determine the crossing points when a full scaling analysis was carried for $\Delta n = 1.66$, 2.25, and $2.80 \times 10^{13} \text{ cm}^{-2}$ using data at many different temperatures. Thus, they are greater than the temperatures at which excess resistance occurs. Because the crossing points were well defined when there were extensive data, one can be confident that the intersection at two temperatures would be a reliable determination of the critical resistance and critical field.

Using both the full scaling analyses and the reduced crossing-point analyses, we were able to map out the variations of both B_c and R_c with Δn as shown in Figs. 10 and 11 respectively. The critical field, B_c , increased with Δn , as $(\Delta n - \Delta n_c)^{0.33}$. Qualitatively, this is what would be expected, since adding carriers strengthens superconductivity and destroying stronger superconductors would require higher magnetic fields. The critical resistance decreased linearly with Δn . Data from the electrostatically tuned transition in a magnetic field of 2.5 T are included on these plots. If these data are excluded, the functional forms are unchanged.

The exponent product νz is the same, within experimental uncertainty, for the parallel magnetic field tuned transitions

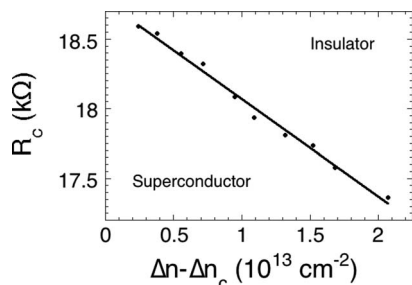


FIG. 11. Phase diagram of R_c vs $(\Delta n - \Delta n_c)$ for the 10.22 Å thick film. The best description is a linear relation.

at various strengths of electrostatically induced superconductivity and the electrostatically-tuned transitions in zero and finite magnetic fields. This suggests that these quantum phase transitions belong to the same universality class and that these phase diagrams demarcate the insulating and superconducting regimes with a robust phase transition line that can be crossed in either direction, by tuning B or Δn . Note that the regime of excess resistance found in parallel magnetic fields may imply that the insulating ground state may be different from that which might be deduced from the analysis of data obtained at high temperatures and used to construct Figs. 10 and 11.

F. Excess resistance in high magnetic fields

In films whose parameters place them on the border between the insulating and superconducting regimes, or well into the insulating regime, we observed behavior in which resistance in magnetic fields became higher at low temperatures than what might have been expected from extrapolation of $R(T)$ at higher temperatures. This regime appears to involve physics that is different from that which determines quantum criticality. While a scaling analysis is successful including data obtained at higher temperatures, it fails when data from this regime is included.

To illustrate this excess resistance, we now discuss in more detail data from the parallel magnetic field-tuned transition shown in Fig. 8. Here, the resistance is larger than what is expected by extrapolating the curves of $R(T)$ down from temperatures in excess of 150 mK. Between 3 T and the parallel critical field of 4.625 T, while superconducting fluctuations cause $R(T)$ curves to head towards zero resistance as temperature is lowered, there is a small upturn in resistance as 60 mK is approached. This upturn in $R(T)$ is found at all higher fields in the insulating regime. It is easily visible at fields between 4.625 T and 7 T, where the upturn occurs simultaneously with a minimum in $R(T)$. In fields in excess of 7 T, there are no minima in $R(T)$ since the general shape is that of an insulating curve with $dR/dT < 0$ for all T , but there is still an excess resistance at low temperatures. Here, resistance is in excess of an extrapolation of Mott VRH, which describes data from 130 mK up to 1 K. To illustrate this, $R(T)$ in fields of 8, 9, and 11 T from Fig. 8 are replotted in Fig. 12 in the form $\ln(R)$ vs $T^{-1/3}$. At higher temperatures, 2D Mott VRH is seen to be a good fit, while below about 130 mK, the resistance becomes greater than extrapolations using the Mott form from higher temperatures.

The minima in $R(T)$ and the increase in resistance at temperatures below those at which the minima occur are both qualitatively similar to features in granular superconducting films. In granular films, minima in $R(T)$ and the subsequent increase of resistance with decreasing temperature are believed to be indicative of persistence of superconductivity on mesoscopic sized grains, where intergranular transport is via single-particle tunneling. We have not observed reentrance in the absence of magnetic field, either in the electrostatically tuned SI transition or the thickness-tuned transition (see Figs.

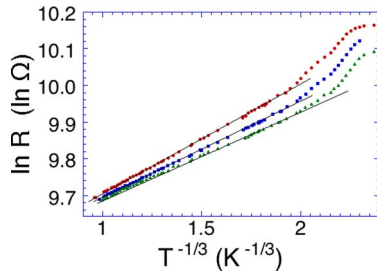


FIG. 12. (Color online) With superconductivity first induced in the 10.22 Å thick film with $\Delta n = 3.35 \times 10^{13} \text{ cm}^{-2}$, $\ln(R)$ vs $T^{-1/3}$ for insulating curves induced by 8 (bottom), 9, and 11 (top) T. The data are fit well by Mott VRH for $T > 150$ mK, but deviates to a higher resistance below 150 mK. Straight lines have been added as guides to the eye.

1 and 2). This suggests that there are no mesoscopic clusters in the film.

The magnitude of the excess resistance in magnetic field in these films is much smaller than that in granular films. For instance, for $B = 8, 9,$ and 11 T, resistances become about 4–8% higher at 65 mK than one would expect from extrapolation. At these fields, the minima occur at about 140 mK. In contrast, in granular films at temperatures a factor of two lower than the temperature at a minimum, resistance is found to be some 16 times higher than is predicted, due to a $(T/T_{min})^4$ dependence associated with the opening of the energy gap as superconductivity develops on the grains.^{48,49}

The highest temperature at which excess resistance is observed in a given field, denoted as T_{onset} , increases with increasing field. This was checked for the four sets of parallel field induced SI transitions for which full scaling analyses were performed, as well as for an intrinsically insulating film where superconductivity was not induced electrostatically. For each superconducting film, the onset of excess resistance appears around the critical magnetic field of the SI transition. As mentioned before, B_c increases with Δn . Interestingly, these $T_{onset}(B)$ curves collapse if shifted horizontally to align the critical fields. This is shown in Fig. 13. This implies that when superconductivity is stronger (at larger Δn) it takes a larger field to induce excess resistance than it takes when superconductivity is weaker (at smaller Δn). It also implies that once excess resistance has been induced, it develops

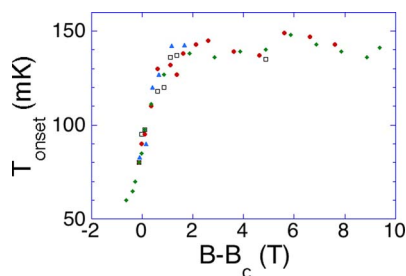


FIG. 13. (Color online) T_{onset} vs $B - B_c$ for superconducting films with various values of Δn . $\Delta n = 1.66$ (diamonds), 2.25 (triangles), 2.80 (squares), and 3.35 (circles) $\times 10^{13} \text{ cm}^{-2}$. The data have been collapsed by shifting these curves by 2, 2.7, 3.5, and 3.75 T, respectively, from the unadjusted values.

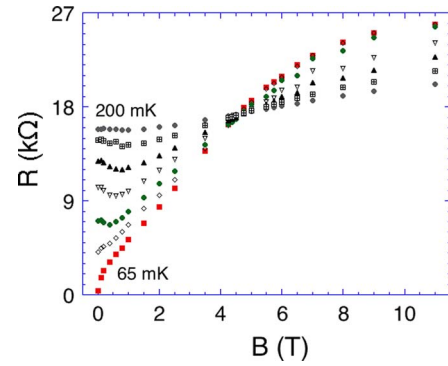


FIG. 14. (Color online) $R(B)$ for the 10.22 Å thick film with $\Delta n = 3.35 \times 10^{13} \text{ cm}^{-2}$. The isotherms correspond to 65, 75, 85, 100, 120, 150, and 200 mK. At high fields, $dR/dB > 0$.

with increasing field in a manner that is independent of the initial strength of superconductivity.

There have been several observations of a peak in the magnetoresistance at fields in excess of the critical field for the SI transition in thicker films (~ 50 – 300 Å) of In_2O_3 and of TiN, both in fields aligned perpendicular^{13,31,32,34–36} to and parallel³⁹ to the film plane. This peak has even been observed in insulating Be films.³⁸ Typically, this resistance peak is found to be larger in films with high normal state resistances (and correspondingly low values of T_c) than in those with low normal state resistances and higher values of T_c .³⁶ When we induce superconductivity in the 10.22 Å thick film with $\Delta n = 3.35 \times 10^{13} \text{ cm}^{-2}$, with $R_N \sim 16 \text{ k}\Omega$ and $T_c \sim 60$ mK, we do not observe a peak in resistance as a function of field. In Fig. 14, we show $R(B)$ for various isotherms between 65 mK and 200 mK. For all isotherms, $dR/dB > 0$ at high fields. This appears to be a general feature of our films, as we observed $dR/dB > 0$ up to 12 T at all temperatures in the other parallel magnetic field tuned transitions at smaller values of Δn and for the insulating films in this sequence.

G. Comparison of the field-tuned SI transitions of intrinsic and electric-field induced superconductors

A separate experiment on parallel field tuning of the SI transition was conducted on an intrinsically superconducting film. The results of a finite size scaling analysis were nearly identical to those found for the transition of an electrostatically-induced superconducting film. The excess resistance in high fields was also nearly identical to that found in an electrostatically-induced superconducting film. The sample was a 10.25 Å thick a -Bi film deposited on top of 10 Å thick a -Sb layer on a STO substrate that had not been thinned. This film was superconducting with a transition temperature $T_c = 130$ mK and a normal state sheet resistance, $R_N \sim 9,500 \Omega$. Parallel magnetic fields induced insulating behavior and finite size scaling was successful over a range of temperatures from 150 to 400 mK. A distinct crossing point was found, with $R_c = 10,460 \Omega$ and $B_c = 9.18$ T. The critical exponent product that produced the best collapse of data was 0.75 ± 0.1 , slightly higher than found for the field-tuned transition of an electrostatically induced superconducting film, but agreeing within the uncertainty. Excess resis-

tance was observed in fields ranging from 8 T to 12 T at temperatures below about 150 mK. At 12 T, a fit to $R(T)$ by Mott VRH was successful down to 150 mK. For data below 150 mK, the excess resistance again prevented successful scaling. For $T > 400$ mK, the negative slope of dR_c/dT prevented successful scaling. At high fields and at all temperatures, dR/dB was always positive.

IV. DISCUSSION

A. Magnetic field alignment

An important technical issue for studies in parallel magnetic fields is the alignment of the plane of the substrate with the field. Our estimate of the maximum angular misalignment of the is 1° . This is based on multiple geometrical constraints. For the magnetic field tuned SI transition for superconductivity induced by adding $\Delta n = 3.35 \times 10^{13} \text{ cm}^{-2}$, the transition temperature is 60 mK, the “mean field” transition temperature is 90 mK, and the critical field is 4.625 T. This critical field is 27 times higher than the limiting value necessary to destroy superconductivity by aligning spins, found by Clogston and Chandrasekhar to be 1.9 T/K. An enhancement of this magnitude might be expected since Bi is a heavy metal with strong spin-orbit interaction and consequently a -Bi would be expected to have a short spin orbit scattering time. At each electron scattering event, the spin flips, leading to a substantially enhanced value of the critical field relative to the Clogston/Chandrasekhar limiting field. If we were to assume that this result was due to a perpendicular field component resulting from misalignment larger than our estimate, a misalignment of about 7 to 11° would be necessary to produce the critical fields in Fig. 10. We base this on comparison with work on similar a -Bi films by Markovic *et al.*²⁰ in which a perpendicular field of 0.6 T was needed to quench superconductivity in a film that has a transition temperature between that found here at $\Delta n = 1 \times 10^{13} \text{ cm}^{-2}$ and $3.35 \times 10^{13} \text{ cm}^{-2}$, based on its shape. This is unreasonably large, given the geometrical constraints.

B. SI transitions

In aggregate, finite size scaling analyses of the various SI transitions tuned by thickness, electrostatic electron doping, and perpendicular and parallel magnetic fields have yielded a wide range of results. Scaling analyses of measurements in which perpendicular magnetic field,^{11,19,20,32,39,50} or thickness²¹ have been tuned have usually resulted in $\nu z \sim 1.3$ and $z=1$, which is consistent both with the scaling theory,⁹ (2+1) dimensional xy model with disorder,⁵¹ and other and numerical studies.⁵²⁻⁵⁷ This value has been suggested to be consistent with percolation.^{23,24} An exception is the case of a -Bi, in which tuning the transition by a perpendicular field has yielded $\nu z \sim 0.7$, while tuning with thickness has yielded $\nu z \sim 1.3$, while a partial electric field scaling analysis has suggested $z=1$.²⁰ This value of ν disagrees with what was believed to be a theorem that predicts $\nu \geq 1$ in two dimensions in the presence of disorder.⁵⁸ The possible irrelevance of this theorem to the SI transition has been discussed most recently by Chamon and Nayak.⁵⁹ The present mea-

surements suggest that transitions tuned by electron doping and parallel magnetic fields have exponent products νz of 0.65 to 0.75. Thus if $z=1$, $\nu=0.7$ is consistent with earlier perpendicular field scaling, as well as numerical studies of the 3D xy model^{7,51} and the Boson-Hubbard models in the absence of disorder.⁶⁰ This is suggestive that thickness-tuned transitions in a -Bi may be percolative, while transitions for other tuning parameters are not.

In the present work, we found that the relation between critical parallel magnetic field and electron density is $B_c \sim (\Delta n - \Delta n_c)^{0.33}$. There appears to be no theory predicting the relationship between Δn and B_c . It appears that the line of criticality can be crossed changing either B or Δn with a finite size scaling analysis yielding the same critical exponent product. This is different than in the work of Markovic *et al.*,²¹ in which the relationship between perpendicular magnetic field and film thickness, d , was found to be $B_c \sim (d - d_c)^{0.7}$ but crossing the phase boundary by tuning B and d produced different critical exponents. In the context of the current experiment, this then appears to further suggest that tuning by changing film thickness in bismuth films is due to percolative effects, while other tuning parameters may not be.

The values of critical resistances for all of the transitions of electrostatically induced superconductivity are a factor of two or three higher than those found in other SI transitions and the universal value of 6455Ω predicted by the dirty Boson model. While the critical resistance has been found experimentally to be nonuniversal,^{11,20} it has been studied in various materials and samples with different levels of disorder. Here, in a sample with a static level of disorder, we have shown the critical resistance decreases linearly with increasing electron density.

Excess resistance appears to be a low temperature feature of films in the insulating regime in the presence of parallel magnetic fields. Fields have produced this both insulating regime when superconductivity was quenched by field and in the intrinsic insulating state. The features of $R(T)$ in parallel magnetic fields are qualitatively similar to features in $R(T)$ in zero field for granular films. The conventional view is that quench-condensed films grown with either a -Ge or a -Sb underlayers are disordered on an atomic rather than a mesoscopic scale. Since these films anneal at temperatures around 25 K, whereupon they change into semimetals, we cannot examine them structurally to determine the level of homogeneity. However, since we have not observed reentrance in the absence of magnetic field, either in the electrostatically tuned SI transition or the thickness-tuned transition, we believe that there are no mesoscopic scale clusters in the film. It is possible that the parallel magnetic field induces spatial inhomogeneity of the amplitude of the superconducting order parameter that mimics clustering.

Flattening of $R(T)$ below about 60 mK in zero magnetic field may only be a consequence of failure to cool the film. In nonzero magnetic field its occurrence at temperatures higher than 60 mK may be due to enhanced Eddy current heating or there may be an intrinsic metallic regime.

Interestingly, we have not observed a peak in the magnetoresistance after superconductivity has been quenched by

magnetic fields, even though our transition temperatures are very low and normal state resistances are very high, which is the regime in which the largest peaks of In_2O_3 films were found.³⁶ We do not find a peak either below 150 mK, in the regime of excess resistance, or above this temperature, where Mott VRH fits well. Though our fields are aligned parallel to the plane of the film, large peaks in magnetoresistance were found by Gantmakher *et al.* in alignments both perpendicular and parallel to the film.^{32,39} Though there is theoretical work suggesting that this metallic regime is intrinsic,²⁷ there have been suggestions that this is a consequence of inhomogeneity in the films.^{35,28} We suggest that further experimental studies of the homogeneity of films exhibiting peaks in magnetoresistance in the presence of large magnetic fields would help resolve the issue of whether these magnetoresistance peaks are intrinsic properties of structurally and chemically homogeneous films.

V. CONCLUSIONS

We have investigated the two-dimensional superconductor-insulator transition in disordered ultrathin α -Bi films by use of electrostatic electron doping using the electric field effect and by the use of parallel magnetic fields. Electrostatic doping was carried out in both zero and nonzero magnetic fields, and magnetic tuning was conducted at multiple strengths of electrostatically induced superconductivity. The various transitions were analyzed using finite size scaling to determine the critical exponent products of the quantum phase transitions, which were all found to be $\nu z = 0.65$ or 0.7 ± 0.1 . The critical parallel magnetic field increased with electron transfer, Δn , as $(\Delta n - \Delta n_c)^{0.33}$, while the critical resistance decreased linearly with electron transfer.

An anomalous regime of excess resistance that is induced by a parallel magnetic field was also observed. This excess resistance was not observed in zero magnetic field for either thickness or electrostatic tuning. The existence of this regime necessitated that data below 100 to 150 mK be excluded in order for scaling to be successful.

Although there is a long history of experimental and theoretical investigation of the control of superconductivity with electric fields beginning with Glover and Sherill,⁶¹ there has been no significant tuning of superconductivity in metallic systems, and models based on the BCS theory⁶²⁻⁶⁴ only treat the effect on the transition temperature of changes in the density of states in response to changes in the carrier concentration. They do not include an issue that is relevant here, the apparent insulator to metal transition that accompanies the superconductor to insulator transition.⁴⁰ The change in

the coefficient of the $\ln(T)$ behavior of the resistance in the normal state reported in Parendo *et al.*⁴⁰ implies that the effective electron-electron interaction is also changed as the carrier concentration (electron density) is increased. This is not included in any of the theoretical treatments and is a challenge for theory.

The parallel field tuned SI transition leads to values of the critical field that are the order of a factor of 30 in excess of the Pauli limiting field for a superconductor with a transition temperature of 60 mK. This is to be expected for a system with strong spin-orbit scattering. In this instance the rather extensive theoretical treatments⁶⁵ of the critical fields of superconductors are not applicable as quantum fluctuations and the fact that the normal phase is an insulator and not a metal have not been taken into account.

Finally the excess resistance in the insulating phase of the parallel field tuned transition, which actually appears like quasireentrant superconductivity, strongly suggests the existence of a regime in which the superconducting order parameter is inhomogeneous even if the film is not mesoscopically clustered, i.e., that there may be superconducting droplets in an insulating matrix. Although this was observed only in the field-tuned transition and not in the electrostatically tuned transition, the idea is fairly generic in theories of SI transitions in homogeneously disordered films. The case of perpendicular fields has been considered by Spivak and Zhou⁶⁶ and by Galitski and Larkin.¹² For thin films with strong spin-orbit scattering, as would be the case for α -Bi, Zhou⁶⁷ has shown that there should be a glassy phase. We have observed very slow relaxation in high magnetic fields, which could be evidence of such a regime. In all instances the inhomogeneous regime is confined to a narrow region around the critical field. Recently Skvortsov and Feigelman⁶⁸ have considered the suppression of superconductivity by disorder in films of high dimensionless conductance. They find an inhomogeneous regime close to the critical conductance where superconductivity is completely suppressed. This is not seen in our electrostatically tuned transition, perhaps due to the relatively low normal state conductance in our films.

ACKNOWLEDGMENTS

The authors would like to thank A. Efros, B. Shklovskii, L. Glazman, A. Kamenev, P. Crowell, J. Meyer, A. Finkel'shtein, and Y. Imry for many helpful discussions. They would also like to thank A. Bhattacharya, M. Eblen-Zayas, and N. Staley for their work with SrTiO_3 substrates that facilitated this research. This research was supported by the National Science Foundation under Grant No. NSF/DMR-0455121.

¹S. L. Sondhi, S. M. Girvin, J. P. Carini, and D. Shahar, *Rev. Mod. Phys.* **69**, 315 (1997).

²S. Sachdev, *Science* **288**, 475 (2000).

³Sadamichi Maekawa and Hidetoshi Fukuyama, *J. Phys. Soc. Jpn.* **51**, 1380 (1981).

⁴D. Belitz, *Phys. Rev. B* **40**, 111 (1989).

⁵A. Finkel'shtein, *Pis'ma Zh. Eksp. Teor. Fiz.* **45**, 37 (1987) [*JETP Lett.* **45**, 46 (1987)]; *Physica B* **197**, 636 (1994).

⁶J. M. Valles Jr., R. C. Dynes, and J. P. Garno, *Phys. Rev. Lett.* **69**, 3567 (1992); S.-Y. Hsu, J. A. Chervenak, and J. M. Valles Jr.,

- Phys. Rev. Lett. **75**, 132 (1995).
- ⁷M. P. A. Fisher, P. B. Weichman, G. Grinstein, and D. S. Fisher, Phys. Rev. B **40**, 546 (1989).
- ⁸M. P. A. Fisher, Phys. Rev. Lett. **65**, 923 (1990).
- ⁹M. P. A. Fisher, G. Grinstein, and S. M. Girvin, Phys. Rev. Lett. **64**, 587 (1990).
- ¹⁰Nandini Trivedi, Richard T. Scalettar, and Mohit Randeria, Phys. Rev. B **54**, R3756 (1990).
- ¹¹A. Yazdani and A. Kapitulnik, Phys. Rev. Lett. **74**, 3037 (1995).
- ¹²V. M. Galitski and A. I. Larkin, Phys. Rev. B **63**, 174506 (2001).
- ¹³T. I. Baturina, J. Bentner, C. Strunk, M. R. Baklanov, and A. Satta, Physica B **359**, 500 (2005).
- ¹⁴M. Strongin, R. S. Thompson, O. F. Kammerer, and J. E. Crow, Phys. Rev. B **1**, 1078 (1970).
- ¹⁵H. M. Jaeger, D. B. Haviland, B. G. Orr, and A. M. Goldman, Phys. Rev. B **40**, 182 (1989).
- ¹⁶D. B. Haviland, Y. Liu, and A. M. Goldman, Phys. Rev. Lett. **62**, 2180 (1989).
- ¹⁷Z. Ovadyahu, Phys. Rev. B **47**, 6161 (1993).
- ¹⁸V. F. Gantmakher, M. V. Golubkov, J. G. S. Lok, and A. K. Geim, JETP Lett. **82**, 951 (1996).
- ¹⁹A. F. Hebard and M. A. Paalanen, Phys. Rev. Lett. **65**, 927 (1990).
- ²⁰N. Markovic, C. Christiansen, A. M. Mack, W. H. Huber, and A. M. Goldman, Phys. Rev. B **60**, 4320 (1999).
- ²¹N. Markovic, C. Christiansen, and A. M. Goldman, Phys. Rev. Lett. **81**, 5217 (1998).
- ²²V. F. Gantmakher, M. V. Golubkov, V. T. Dolgoplov, G. E. Tsydynzhapov, and A. A. Shashkin, JETP Lett. **71**, 160 (2000).
- ²³E. Shimshoni, A. Auerbach, and A. Kapitulnik, Phys. Rev. Lett. **80**, 3352 (1998).
- ²⁴Yigal Meir, Phys. Rev. Lett. **83**, 3506 (1999).
- ²⁵N. Mason and A. Kapitulnik, Phys. Rev. B **64**, 060504(R) (2001).
- ²⁶Kevin A. Parendo, L. M. Hernandez, A. Bhattacharya, and A. M. Goldman, Phys. Rev. B **70**, 212510 (2004).
- ²⁷V. M. Galitski, G. Refael, M. P. A. Fisher, and T. Senthil, Phys. Rev. Lett. **95**, 077002 (2005).
- ²⁸I. S. Beloborodov, Ya. V. Fominov, A. V. Lopatin, and V. M. Vinokur, cond-mat/0509386 (unpublished).
- ²⁹Denis Dalidovich and Philip Phillips, Phys. Rev. B **64**, 052507 (2001); Denis Dalidovich and Philip Phillips, Phys. Rev. Lett. **89**, 027001 (2002).
- ³⁰C. Christiansen, L. M. Hernandez, and A. M. Goldman, Phys. Rev. Lett. **88**, 037004 (2002).
- ³¹M. A. Paalanen, A. F. Hebard, and R. R. Ruel, Phys. Rev. Lett. **69**, 1604 (1992).
- ³²V. F. Gantmakher, M. V. Golubkov, V. T. Dolgoplov, G. E. Tsydynzhapov, and A. A. Shashkin, JETP Lett. **68**, 363 (1998).
- ³³V. F. Gantmakher, S. N. Ermolov, G. E. Tsydynzhapov, A. A. Zhukov, and T. I. Baturina, Zh. Eksp. Teor. Fiz. **77**, 498 (2003) [JETP Lett. **77**, 424 (2003)].
- ³⁴N. Hadacek, M. Sanquer, and J.-C. Villegier, Phys. Rev. B **69**, 024505 (2004).
- ³⁵G. Sambandamurthy, L. W. Engel, A. Johansson, and D. Shahar, Phys. Rev. Lett. **92**, 107005 (2004).
- ³⁶Myles Steiner and Aharon Kapitulnik, Physica C **422**, 16 (2005).
- ³⁷T. Wang, K. M. Beauchamp, A. M. Mack, N. E. Israeloff, G. C. Spalding, and A. M. Goldman, Phys. Rev. B **47**, 11619 (1993).
- ³⁸V. Y. Butko and P. W. Adams, Nature (London) **409**, 161 (2001).
- ³⁹V. F. Gantmakher, M. V. Golubkov, V. T. Dolgoplov, A. A. Shashkin, and G. E. Tsydynzhapov, JETP Lett. **71**, 473 (2000).
- ⁴⁰Kevin A. Parendo, K. H. Sarwa B. Tan, A. Bhattacharya, M. Eblen-Zayas, N. E. Staley, and A. M. Goldman, Phys. Rev. Lett. **94**, 197004 (2005).
- ⁴¹A. Bhattacharya *et al.*, Appl. Phys. Lett. **85**, 997 (2004).
- ⁴²L. M. Hernandez and A. M. Goldman, Rev. Sci. Instrum. **73**, 162 (2002).
- ⁴³A. B. Zorin, Rev. Sci. Instrum. **66**, 4296 (1995).
- ⁴⁴F. C. Wellstood, C. Urbina, and John Clarke, Phys. Rev. B **49**, 5942 (1994).
- ⁴⁵W. Buckel, Z. Phys. **154**, 474 (1959).
- ⁴⁶J. Kakalios, J. Non-Cryst. Solids **114**, 372 (1989).
- ⁴⁷A. Efros and B. I. Shklovskii (private communication).
- ⁴⁸C. J. Adkins, J. M. D. Thomas, and M. W. Young, J. Phys. C **13**, 3427 (1980).
- ⁴⁹G. Eytan, R. Rosenbaum, D. S. McLachlan, and A. Albers, Phys. Rev. B **48**, 6342 (1993).
- ⁵⁰E. Bielejec and W. Wu, Phys. Rev. Lett. **88**, 206802 (2002).
- ⁵¹Min-Chul Cha and S. M. Girvin, Phys. Rev. B **49**, 9794 (1994).
- ⁵²M. Makivic, N. Trivedi, and S. Ullah, Phys. Rev. Lett. **71**, 2307 (1993).
- ⁵³M.-C. Cha, M. P. A. Fisher, S. M. Girvin, M. Wallin, and A. P. Young, Phys. Rev. B **44**, 6883 (1991).
- ⁵⁴E. S. Sorensen, M. Wallin, S. M. Girvin, and A. P. Young, Phys. Rev. Lett. **69**, 828 (1992); M. Wallin, E. S. Sorensen, S. M. Girvin, and A. P. Young, Phys. Rev. B **49**, 12115 (1994).
- ⁵⁵K. G. Singh and D. S. Rokhsar, Phys. Rev. B **46**, 3002 (1992).
- ⁵⁶L. Zhang and M. Ma, Phys. Rev. B **45**, 4855 (1992).
- ⁵⁷Igor F. Herbut, Phys. Rev. Lett. **81**, 3916 (1998).
- ⁵⁸J. T. Chayes, L. Chayes, D. S. Fisher, and T. Spencer, Phys. Rev. Lett. **57**, 2999 (1986).
- ⁵⁹Claudio Chamon and Chetan Nayak, Phys. Rev. B **66**, 094506 (2002).
- ⁶⁰J. Kisker and H. Rieger, Phys. Rev. B **55**, R11981 (1997).
- ⁶¹R. E. Glover and M. D. Sherill, Phys. Rev. Lett. **5**, 248 (1960).
- ⁶²P. Lipavsky, K. Morawetz, J. Kolacek, and T. J. Yang, Phys. Rev. B **73**, 052505 (2006).
- ⁶³B. Ya. Shapiro, Solid State Commun. **53**, 673 (1985); and references cited therein.
- ⁶⁴W. D. Lee, J. L. Chen, T. J. Yang, and B.-S. Chiou, Physica C **261**, 167 (1996).
- ⁶⁵P. Fulde, Adv. Phys. **22**, 667 (1973).
- ⁶⁶B. Spivak and F. Zhou, Phys. Rev. Lett. **74**, 2800 (1995).
- ⁶⁷F. Zhou, Int. J. Mod. Phys. B **113**, 2229 (1999).
- ⁶⁸M. A. Skvortsov and M. V. Feigel'man, Phys. Rev. Lett. **95**, 057002 (2005).